

Accepted manuscript

As a service to our authors and readers, we are putting peer-reviewed accepted manuscripts (AM) online, in the Ahead of Print section of each journal web page, shortly after acceptance.

Disclaimer

The AM is yet to be copyedited and formatted in journal house style but can still be read and referenced by quoting its unique reference number, the digital object identifier (DOI). Once the AM has been typeset, an ‘uncorrected proof’ PDF will replace the ‘accepted manuscript’ PDF. These formatted articles may still be corrected by the authors. During the Production process, errors may be discovered which could affect the content, and all legal disclaimers that apply to the journal relate to these versions also.

Version of record

The final edited article will be published in PDF and HTML and will contain all author corrections and is considered the version of record. Authors wishing to reference an article published Ahead of Print should quote its DOI. When an issue becomes available, queuing Ahead of Print articles will move to that issue’s Table of Contents. When the article is published in a journal issue, the full reference should be cited in addition to the DOI.

Accepted manuscript
doi: 10.1680/jgrma.18.00060

Submitted: 10 July 2018

Published online in 'accepted manuscript' format: 14 December 2018

Manuscript title: A Green Reduction of Graphene Oxide and Enormous Applications in Electric and Bio-Materials

Authors: Ujwala S. Tayade¹, Amulrao U. Borse¹, Jyotsna S. Meshram²

Affiliations: ¹Kavayitri Bahinabai Chaudhari North Maharashtra University, Jalgaon, India.

²Rashtrasant Tukadoji Maharaj Nagpur University, Nagpur, India.

Corresponding author: Jyotsna S. Meshram, Rashtrasant Tukadoji Maharaj Nagpur University, Nagpur, Maharashtra 440033, India. Tel.: 9822937078

E-mail: drjmeshram@gmail.com

Abstract

Herein, we have developed an efficient green reduction method for the reduction of graphene oxide by using seed extract from easily available and cheap plant *Punica grantum* L. seed (Pomegranate). Phytochemical constituents present in the extract are responsible for reduction, stabilization and capping of reduced graphene. The number of methods reported for the physical and chemical reduction of graphene oxide but the green reduction approach now a day become more popular. The *Punica grantum* L seed extract utilized for the reduction of graphene oxide is first time reported. The method is essential because the simple reaction setup, less time-consuming, non-toxic and mild reducing agent and very good yield obtained. The reduction of graphene oxide is confirmed by the different characterization techniques such as Raman spectroscopy, X-ray diffraction, Fourier transform infrared spectroscopy, UV-Visible spectroscopy, Thermogravimetric analysis, and its morphology study by using Scanning and Transmission electron microscopy. The resultant reduce graphene and graphene oxide nanosheets shows the stable dispersion in water and other solvents which implies it to band gap study opening in the electronic field application. The reduced graphene oxide shows biocompatibility and excellent radical scavenging activity against 2, 2-diphenyl-1-picrylhydrazyl (DPPH) free radicals.

1. Introduction

Among various carbon-containing materials, graphene has attracted the tremendous attention of researchers, because of stable 2D morphology and exceptional electronic properties related to its crystal structure.¹⁻³ Nowadays, graphene opens the new era in the field of nanotechnology and having various emerging applications. Some remarkable thermal, electrical, and mechanical properties of graphene responsible for exploited in various fields, such as sensors, solar cells,⁴ nano-electronics,⁵ energy storage,⁶ functional nanocomposites,^{7,8} biomedicine,⁹ and catalysis,¹⁰ etc. Generally, graphene is obtained from graphite,¹¹ which is a natural source of material and widely used from the last few centuries. The report found on free-standing single-layer of graphene was first obtained in 2004 by the isolation of graphene from graphite via micromechanical cleavage. This attractive approach of formation of graphene layers from graphite can only be used for fundamental science and is not suitable for the large-scale production of graphene.¹² Therefore, to overcome this problem more attention is being paid to discover various alternative approaches for the low-cost and bulk production of graphene reported till the date.¹³ In case of production of graphene material, oxidation is the first step which is easily carried out by using a chemical oxidizing agent as a cheap source and the reduction is another method which can apply variable methods for reductions such as mechanical,¹ chemical vapor deposition,¹⁴ epitaxial growth,¹⁵ chemical,^{9,16,17} thermal,⁴ electrochemical, photochemical methods,^{18,19} and greener approach etc.^{20,21} Out of this the chemical reduction of graphene oxide (GO) is considered the most promising route for a large-scale production at a low cost.²² In chemical method reducing agents such as hydrazine,

sodium borohydride, hydroquinone, hydraulic acid or formamidine sulfonic acid have been applied for the reduction of GO to reduced graphene oxide (GR).²³⁻²⁵ But the chemical reducing agent, such as hydrazine, is hazardous and harmful to both human life and the environment. Many time chemical methods are responsible for “doping” with other elements (nitrogen in the case of hydrazine), which results in changing of the electronic properties of graphene.²⁶ The chemically reduced GO sheets have a strong tendency to undergo irreversible agglomeration and precipitation due to π - π stacking, which is avoided by the addition of chemical stabilizers such as porphyrin, pyrene butyric acid, or poly (oxy alkyne) amines.^{27, 28}

By considering, above mentioned challenges innovative approach needful to develop that makes use of eco-friendly reducing agents for the production and stabilization of reduced graphene oxide (GR). Therefore, natural products, including Gallic acid, L-lysine, Melatonin, L-ascorbic acid, green tea and wild carrot roots have been developed for the preparation of GR.²⁹⁻³² Plant extracts are relatively easy to handle, readily available, low cost as compared to any other source and due to their biocompatibility in the field of nanotechnology, they are widely used. In the case of nanoparticles synthesis mostly plant extract was reported as reducing and stabilizing agent,³³⁻³⁹ but in the reduction of graphene oxide is not common.

In the present work, we highlighted a simple and environment-friendly approach for the preparation of GR using an extract of *Punica grantum L.* seeds this was explained in Figure.1. The extract not only acts as bio-reductants but also functionalizes the surface of the GR nano-sheets. The preparation of seed extract is simple as compared to other extraction processes. The extract applications were reported in the food colorant, medicinal application,

dye-sensitized solar cells etc. But in the present work it acts as efficient reducing and capping agent provided no need of controlled reaction parameters, the addition of extra chemicals, reaction setup is also very simple and results in higher yield. The cost-effectiveness of the process, defect-free graphene i.e. no aggregation in the nanosheets, formation of stable dispersion are the key features of work. We have also studied the effect of the solvent dependent study of the dispersion of GO and reduced GR as well as calculated its band gap. Also, the antioxidant study by using 1, 1-Diphenyl-2-picrylhydrazyl (DPPH) assay for GO and GR. The nanosheet formation was confirmed by using various characterization techniques such as X-ray powder diffraction (XRD), Fourier-transform infrared (FT-IR) spectroscopy, Fourier-transform Raman (FT-Raman) spectroscopy, Ultraviolet-visible absorption (UV-Vis) spectroscopy, Thermogravimetric analysis (TGA), Fluorescence measurement, Scanning electron microscopy (SEM) and Transmission electron microscopy (TEM) with SAED pattern.

2. Experimental

2.1 Materials

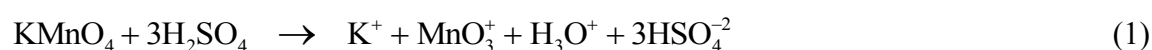
Pomegranates were purchased from the local market, Concentrated HCl, Ethanol (98%) pure, Graphite powder (99.999 %, - 60 mesh), Concentrated sulfuric acid (H₂SO₄, 98 %), Potassium permanganate (KMnO₄, 99 %), Sodium nitrate (NaNO₃, 99 %) and Hydrogen peroxide (H₂O₂, 30 %) and all organic solvents were obtained from Aldrich Chemicals (USA) and used without further purification.

2.2 Preparation of graphene oxide by Hummers method from graphite

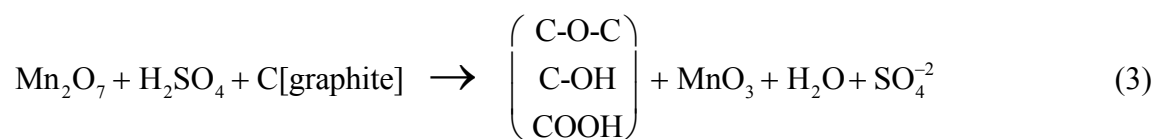
The 2 g graphite powder was added to 46 mL of concentrated H₂SO₄ (in an ice bath) simultaneously, the addition of 6 g KMnO₄ gradually (maintained the temperature of the solution to 20 °C). The resulting mixture was stirred for 2 h. The temperature was then allowed to increase up to 35 °C and the suspension was stirred for an additional 2 h. In the end, 92 mL of deionized water was added slowly to the solution. After 1 h, the mixture was diluted further with 280 mL of deionized water. Then 10 mL of H₂O₂ (30 %) was added slowly which results in an appearance of vigorous bubbles and a change in the color of the suspension from deep brown to yellow were observed. The suspension could settle for at least one day, after which the clear supernatant was decanted, the remaining suspension was filtered and washed with 5% HCl solution and acetone, followed by several washes with deionized water to remove the traces of acid. The resultant graphene oxide paste was dried for one day.⁴⁰

2.3 Formation mechanism of graphene oxide

In the graphene oxide formation mechanism involves, the active species to oxidize graphite is diamanganese heptoxide (Mn₂O₇) which is obtained via the reaction of monometallic tetroxide and MnO₃⁺ as shown in the following reaction (1) and (2).^{41, 42}



The transformation of MnO₄⁻ into a more reactive form Mn₂O₇ will certainly help oxidize graphite powder as shown in the reaction below (3).^{43, 44}



But the bimetallic form of manganese oxide has been reported to donate electron when heated up to 55 °C temperature or when reacted with organic compounds.²⁷

2.4 Preparation of *Punica grantum L* seed extract

The pomegranates were washed with tap water and manually separated into seeds. The seeds are thoroughly washed with deionized water, crushed with mortar and piston, the pulp formed was added in 1% HCl-Ethanol, followed by constant stirring for proper mixing of pulp in the system, the vessel containing pulp was covered and kept for 12 h in a freezer. The frozen sample was then kept for 20-30 min at room temperature and filtered by using what man filter paper. Again, the filtrate was collected and centrifuged at 3000 rpm to remove any solid impurity present in the extract. The prepared extract was stored at 4 °C for further experiment. To determine the exact phytochemicals, present in the extract the phytochemical screening test performed which are responsible for the reduction and capping of graphene oxide shown in table no.1.

2.5 Preparation of reduced graphene oxide by *Punica grantum* extract

The graphene oxide (200 mg) was first dispersed in 40 mL of deionized water and sonicated for 30 min to obtain graphene oxide (GO) sheets. The resulting suspension was heated to 100 °C; 10 mL of an aqueous solution of the plant extract (0.4 g ml⁻¹) was added to the suspension, which was then allowed to stir for 8 h at 98 °C. The *Punica grantum L.* based GR

nanosheet was collected by filtration method using what man filter paper no. 41 as a black powder. The collected black powder washed with distilled water several times to remove the excess plant extract residue and redistributed into the water for sonication. This suspension was centrifuged at 4000 rpm for another 30 min and the final product was collected by vacuum filtration.

2.6 DPPH radical scavenging assay

1, 1-Diphenyl-2-picrylhydrazyl (DPPH) is a well-known stable free radical, the natural antioxidant free radical scavenging activity of DPPH assay was determined. ⁴⁵ GO and GR concentrations of (50–200 µg/mL) were added, at an equal volume of a methanolic solution of DPPH. The mixture could react at room temperature in the dark for 30 min. Ascorbic acid was used as a standard control. The optical density of DPPH radical is monitored. After 30 min, the absorbance (A_1) was measured at 518 nm and converted into the percentage of antioxidant activity using the following equation:

$$\% = [(A_0 - A_1)/A_0] \times 100$$

Where, A_0 -was the absorbance of the control and A_1 -was the absorbance in the presence of composite.

3. Characterization of reduced graphene oxide

3.1 *UV-Visible spectroscopy*

A Carrey win (USA) UV-Visible spectrophotometer was used for the optical measurements. The analysis was performed in quartz cuvettes using deionized water as a reference solvent. UV-Visible spectrums scan in the range of 200-800 nm at room temperature.

3.2 *Fourier transform infrared spectroscopy*

Fourier Transform Infrared spectra were measured on a Shimadzu (1700). The samples were mixed with KBr powder and pressed into a pellet for measurement. Background correction was made using a reference KBr pellet. FT-IR spectrums scan in the range of 400 cm^{-1} to 4000 cm^{-1} at room temperature.

3.3 *High-performance liquid chromatography*

Separation and identification of anthocyanin were carried out by HPLC modifications. The HPLC system consisted of a SIL-10AD VP auto-injector (Shimadzu), SCL-10A VP system controller (Shimadzu), LC-10AT VP liquid chromatograph (Shimadzu). Samples were diluted in water and filtered prior to injection. 50 μL of each extract was injected onto a Luna C₁₈ column, 4.6 -250 mm (Phenomenex, Australia), kept at 25°C, with a binary mobile phase of A: 9% Acetonitrile, 10% formic acid and B: 36% Acetonitrile, 10% formic acid. Samples were eluted under isocratic conditions at a flow rate of 1.0 mL/min and were monitored at 520 nm with a run time of 50 min for each sample.

3.4 X-ray diffraction

X-ray diffraction (XRD) patterns were recorded using a Rigaku Rota flex RU-200B diffractometer with a $\text{CuK}\alpha$ ($\lambda = 1.5418\text{\AA}$) in the scanning angle of 20 to 80 degrees.

3.5 Raman spectroscopy

Raman spectra were recorded on a Horiba JY Lab RAM HR800 micro-Raman spectrometer equipped with 17 mW 632.8 nm laser excitation (He–Ne laser, E laser = 1.96 eV) in the backscattering mode.

3.6 Thermogravimetric analysis

The weight loss of the samples was collected by TGA thermal analyzer (Perkin Elmer 4000) in range of temperature from 50 to 900 °C at a heating rate of 10 °C/min in a nitrogen atmosphere.

3.7 Fluorescence measurement

The fluorescence spectra were recorded on a Horiba Jobin Yvon Fluoromax-4 spectrofluorometer at room temperature using a 1-cm sample cell.

3.8 Scanning electron microscopy

Surface morphological studies were performed by using a scanning electron microscope (FE-SEM) unit (S-4800 instrument from Hitachi, Japan) operated at 15.0 kV.

3.9 Transmission electron microscopy

TEM grids were prepared by placing a drop of graphene materials dispersion on a lacy carbon support grid and allowing it to dry in air. TEM images and selected area electron diffraction (SAED) patterns were also taken. For SAED a 0.5 μm aperture was used, with a small spot size and spread beam to increase the electron coherence length at the sample. Low-temperature measurements were performed using a liquid nitrogen cooled sample holder. Unless otherwise specified, images and diffraction patterns were taken at 200kV.

4. Results and discussion

In the present work, extract acts as a reducing agent in graphene oxide and the mechanism of reduction may follow the given pathway.

The phytochemicals present in the extract as shown in Table 1 are carbohydrates, glycosides, flavonoids, phytosterols, protein etc. which are responsible for the reduction and stabilization of GR.

The visual observations show that GO dispersion was brownish yellow while the reduction of GO with *Punica grantum* L seeds resulted in a black dispersion. This is attributed to a result of an increase in the hydrophobicity of the material caused by a decrease in oxygen-containing functional groups (removal of most of the functional groups) present on the surface of GO sheet materials. ⁴⁶

4.1 Plausible mechanism of reduced graphene oxide by anthocyanin

In this mechanism the possibility of epoxy groups of GO can be easily attacked by nucleophilic reagents, resulting in a nucleophilic substitution reaction to open the epoxy rings.⁴⁷ It is supposed that polyphenols (anthocyanine) donate an electron to graphene oxide (generally reducing agent is that can able to donate an electron to an oxidized substance for reduction purpose). It opens the epoxide rings and converts to easily/ good leaving group (OH) and finally, removal of water molecule takes place, leaving a reduced graphene sheet. To remove the OH group it is supposed that anthocyanine donates one proton to the OH group and finally dehydrates this mechanism is shown in Figure 2.

4.2 UV-Visible spectroscopy and bandgap calculation

Graphene oxide reduction was initially monitored by recording UV-Visible absorption spectra of graphene oxide (GO), *Punica grantum L.* seed extract (PE) and reduced graphene oxide (GR) as shown in (Figure 3). GO exhibited absorption peak at 230 nm which was attributed to the $\pi-\pi^*$ transitions of the aromatic C–C bonds and a weak shoulder at 301 nm due to $n-\pi^*$ transitions of C=O bonds present in GO. However, on a reduction of GO to GR, the characteristic absorption band at 301 nm disappeared and the absorption band at 230 nm in GO spectrum is red-shifted to 280 nm in GR, which confirms the reduction of GO and the partial restoration of π network of GR. The higher redshift in case of GR is attributed to the superior degree of reduction compared to GO. The phytochemicals of *Punica grantum L.* seed extract not only reduce the GO but also stabilizes the GR nanosheets. This was confirmed in the previous study by the UV analysis of HRG obtained via reduction of GO using Pulicaria

glutinosa plant extract.⁴⁸ In order to examine the ability of reduction, the UV spectrum of *Punica grantum L.* seed extract was measured, where the absorption maximum appeared at ~282 nm, which overlapped with the characteristic peak of GR (~280 nm).

The UV-Visible spectra help to plot the taucs plot which is used for the calculation of band gap (Figure.4). The GO shows the band gap value 5.1 eV and GR show the band gap value of 4.8 eV. The detailed information provided in the supplementary file.

4.3 Fourier transforms –infrared spectroscopy

The FTIR measurements were carried out to identify the natural products of *Punica grantum L.* seed extract, graphite powder, graphene oxide and reduce graphene oxide.

The FT-IR spectrum of graphite powder and GO contains several bands that indicate the presence of oxygen-containing functional groups like carbonyl, carboxylic, epoxy and hydroxyl (Figure 5 a, b). The reduced intensities of the bands at 3259, 1978, 1724, 1605, 1219 and below 1000 cm⁻¹ associated with these oxygen-containing functional groups indicate the reduction of the GO, i.e. the number of oxygen-containing functional groups decreased significantly after the reduction (Figure 5c). The complete disappearance of -COOH and -OH frequency observed in the GR nanosheets.⁴⁹⁻⁵¹ However, some of the bands observed in the spectrum of GR could be due to the presence of phytochemicals because it stabilizes the surface of GR nanosheets. This was confirmed by a comparison of the IR spectra of GR and the pure *Punica grantum L.* seed extract (PE) (Figure 5 d). Most of the absorption bands due to PE also appear in the FT-IR spectrum of GR. This strongly suggests that the phytochemicals of PE not only act as bio-reductants but also act as stabilizers by adsorbing on the surface of GR

nanosheets. Notably, the absence of absorption bands at 1392 and 1270 cm^{-1} associated with the phenolic OH groups in the FT-IR spectrum of GR (present in the spectrum of seed extract due to phenolic OH) suggest that a possible reduction of GO is carried out by the phenolic OH groups of polyphenols and other constituents (anthocyanin).

4.4 High-performance liquid chromatography

To determine the purity of *Punica grantum L* seed extract and analysis of phytoconstituents present in extract HPLC carried out. In the HPLC results the two major anthocyanins corresponding to peaks 1 and 2 (Figure 6) represented about 70.72% and 29.273%, respectively, of the total peak area revealed at 520 nm. Retention time observed at 6.329 minutes is matched with Pelargonidin-3-glucoside.⁵² Also the broad peak of retention time at 9.058 shows the presence of 9.2 min was identified as cyanidin 3-*O*-galactoside and 9.5 minutes was therefore identified as petunidin 3-*O*-glucoside.⁵³ from these results we can say that the extract is purified no impurity observed in it.

4.5 XRD analysis

The XRD analysis was performed to confirm the crystallinity of graphite powder to GO and its *Punica grantum L* seed extract-forms de-oxygenation to GR. The graphite powder shows a sharp diffraction peak at $2\theta = 25.6^\circ$ (Figure 7 a) corresponds to d-spacing 3.47 Å. However, oxidation of graphite powder involves insertion of oxygen-containing groups, mainly carboxylic acid at the periphery, epoxide and hydroxyl groups between the planes, which leads to an increase in d-spacing to 9.38 Å with the diffraction peak at $2\theta = 9.41^\circ$ ²⁸ (Figure 7 b).

The seed extract-induced de-oxygenation of GO makes this peak at $2\theta = 9.41^\circ$ disappear, indicating the complete reduction of GO to GR nanosheet. In the case of plant extract based reduced graphene oxide, amorphous spectrum (Figure 7c) observed because of phytoconstituents accumulated on the surface of graphene. It is useful to mention here that the XRD mainly reflects the inter-plane spacing and hence the term complete reduction refers primarily to inter-plane oxygen group formation.

4.6 Raman analysis

Raman spectroscopy is an excellent tool to distinguish defective and defects free graphitic forms. The Raman spectra of graphite powder, GO, GR nanosheet samples are shown in (Figure 8). The characteristic peaks of graphitic forms observe in Raman spectra are the G band (assigned to the E_{2g} phonon of sp^2 carbon atoms) and the D band (assigned to the breathing mode of k-point phonons of A_{1g} symmetry).⁹ The spectrum of graphite powder (Figure 8 a) shows strong G band at 1530 cm^{-1} , a tiny D band at 1293 cm^{-1} and a sharp 2D band at $\sim 2578\text{ cm}^{-1}$. However, due to stress, the spectra of GO (Figure 8 b) show broadened G band 1600 and D band 1335 with the blue shift in Raman frequency as compared to the graphite G band. In case of GR (Figure 8 c), the value of G band is again shifted to 1300 cm^{-1} and D band 1564 cm^{-1} . On the other hand, the intensity of D band in all cases except graphite is considerably higher, indicating the decrease in the average size of the in-plane sp^2 domain. It can be inferred that in terms of defects *Punica grantum L.* extract produces higher quality graphene nanosheets from GO as compared to chemical method. This could possibly be

attributed to the milder nature of the green processing approach over the aggressive nature of the chemical processing.

4.7 Thermogravimetric analysis

Thermal degradation or stability of the graphite powder (G), graphene oxide (GO), reduced graphene oxide (GR) and *Punica grantum L* seed extract (PE) was investigated by TGA. (Figure 9 a) shows that G is thermally stable at a temperature below 600 °C and only exhibits one clear step of 4% weight loss above 600 °C. GO was thermally decomposed in the following three steps. A significant weight loss observed at 100 °C, responsible for the removal of adsorbed water molecules due to the hydrophilic nature of GO. At 200 °C, a notable weight loss, responsible for the decomposition of oxygen-containing functional groups present on the GO surface, was observed. The weight loss of GO at above 350 °C is attributed to the decomposition of more stable oxygen-containing functional groups to CO and CO₂. As shown in (Figure 9 a), the GR shows very low weight loss as compared to that of GO over the entire temperature range (50 °C to 900 °C); however, it is still higher than the weight loss of the G, indicating that GR has slightly more oxygenated functional groups than the G, but the fraction of oxygen-containing functional groups in GR is much smaller than in GO.⁵⁴

In case of *Punica grantum L*. seed extract (PE) thermal analysis shown in (Figure 9 b) that the three different degradation steps observed out of which first is related to the loss of water near about 100-200 °C. The degradation between 200-327 °C related to the sugars degradation of extract. In case of the last step of degradation from 346.60-594.01 °C remaining phytochemicals (polyphenols) completely degraded up to 600 °C.⁵⁵

4.8 Fluorescence measurement

The fluorescence/photoluminescence (PL) spectrum of GO and GR nano-sheets shows that PL emission maximum peak is at 485 and 480 nm for the excitation wavelength of 220 nm, as shown in the figure provided in the supplementary file. The photoluminescence emission of GO and GR nano-sheets is observed sp^2 these originate from the recombination of electron-hole pairs, localized within small carbon clusters sp^3 embedded within the matrix.⁵⁶ The PL spectrum of nano-sheets shows PL emission in visible range which could be more applicable in different branches of science and technology also for fluorescence quenching purposely.⁵⁷

4.9 Scanning electron microscopy

The morphology of the samples was studied using FE-SEM. As shown in (Figure 10 (a)), graphite powder shows the platelet-like crystalline form of carbon. After acid treatment, oxidation and ultra-sonication, GO sheets become smaller and transparent in Figure 10 (b). The sheet is become very thin in case of reduced graphene oxide by using plant extract that electron beam can be passed through the sample. Figure 10 (c) and 10 (d) show the particle size of nanosheet of GR in SEM. The folding of nanosheet nature highlighted in the given figure. The average particle size in nanosheet is 33 nm calculated and 16.5 nm is also observed in structure. Some wrinkles were also detected, due to the randomly aggregated and crumpled thin nano-sheets.⁵⁸ They rippled and entangled with each other. They were transparent and stable under the electron beam, which confirmed the existence of two-dimensional nanosheets of GO.

4.10 *Transmission electron microscopy*

The morphology and structure of the graphite powder, graphene oxide, and reduced graphene oxide were studied by transmission electron microscope (TEM) analysis and selected area of the electron diffraction (SAED) pattern of the all respectively presented in Figure 11 (a) shows large graphite sheets which can be observed on the top of the lacy grid and SAED pattern shows the crystalline nature. Different from bulk GO sheets in Figure 11 (b) these layered and aggregated sheets observed and SAED pattern shows the amorphous nature. The reduced graphene oxide, GR sheets, are no longer totally flat and smooth but always exhibit some corrugation, where they resemble crumpled silk veil waves. Especially, any area of the nanosheets shows considerable folding Figure 11 (c) and SAED pattern show again amorphous nature. As previously reported,⁵⁹ this phenomenon is because the thermodynamic stability of the 2D membrane results from microscopic crumpling via bending or buckling. This phenomenon also supports the fact that the coarse aggregates have been exfoliated completely. The SAED pattern not only shows the nature of materials but also helps in the correlation of inter planer structures observed in the XRD spectrum. In case of greener reduction approach the morphology, changes are noticeable, thin and less aggregation.

4.11 *DPPH radical scavenging activity of graphene oxide and reduced graphene oxide*

1, 1-Diphenyl-2-picrylhydrazyl (DPPH), a stable free radical molecule, with absorption at 518 nm by UV–Visible spectroscopy, was used for the radical scavenging effects. The antioxidant activity of the graphene material neutralized the free radical of DPPH by easily transferring an

electron or hydrogen atom to DPPH⁶⁰ to become a yellow colored stable diamagnetic molecule, another important advantage of DPPH radical is, it cannot be affected by side reactions i.e., metal chelation, enzyme inhibition.⁶¹ The de-coloration indicated the scavenging potential of the graphene material. The radical scavenging activity of the GO and GR was determined by the ratio percentage of the sample absorbance decrease, with the absorbance of the DPPH solution without a test sample at 518 nm as explains previously. In this study, it is proved that graphene material effective at inhibiting the DPPH which is mainly recognized to charge transfer of an electron.^{62,63} Figure 12 shows the DPPH free radical scavenging activity [%] of GO and GR, along with ascorbic acid as a standard. In this Figure 12, the standard error bar with 5% used to explain the antioxidant activity. An inhibition property of GR is more as compare to GO because of several functional groups presents on the surface of GO so it slowly reacts. The linear relationship in an activity of both shown in the supplementary file Figure (a) GO and (b) GR. The regression value and straight-line equation used to calculate the IC₅₀ value. The IC₅₀ value of the GO is 142.8 µg/mL and GR is 184.7 µg/mL respectively, the graphene material scavenged 50% of the DPPH radical within the minimum concentration, and this indicated that GR and GO both are an effective antioxidant.

5. Conclusion

The *Punica grantum L.* seed extract employed for the reduction of graphene oxide is very simple, cost-effective, less time consuming and eco-friendly in nature. Non-hazardous chemicals and solvents used in the synthesis. The seed extract is studied for qualitative and quantitative analysis. For the qualitative determination phytochemicals screening performed

and quantitative analysis such as HPLC, Thermogravimetric analysis carried out. The bio reduction was confirmed by using UV-visible, FT-IR, Raman spectroscopy, Thermogravimetric analysis, Fluorescence measurement, XRD analysis, FE-SEM and TEM analysis for morphological changes. The morphology obtained in reduced graphene oxide is more applicable in the electronic field because new band gap opening observed in the dispersions form. Also, the thin nanosheets obtained provides large surface area and acts as good antioxidant material against DPPH free radicals, the regression values show it. The *Punica grantum L.* seed extract acts as best reducing and stabilizing agent because no aggregation observed in nanosheets morphology. The Raman spectroscopy confirms that the present green reduction forms defect-free graphene nanosheets as compare to the chemical and electrical method. In the SEM analysis, it is observed that the average size is 33 nm. The fluorescence study shows that it can act as a fluorescence quenching agent and bioimaging of molecules. Considering the number of merits and properties of reduced graphene oxide and simplicity of reaction conditions it can be applied in large-scale production.

Acknowledgements

One of the authors, Miss. Ujwala Sakharam Tayade acknowledges Shri. G. H. Raisonni Doctoral Fellowship for financial support.

References

1. Novoselov KS, Geim AK, Morozov SV, Jiang DA, Zhang Y, Dubonos SV, Grigorieva IV, Firsov AA. (2004) Electric field effect in atomically thin carbon films. *Science* **306**:666-669.
2. Rao CE, Sood AE, Subrahmanyam KE, Govindaraj A. (2009) Graphene: the new two-dimensional nanomaterial. *Angewandte Chemie International Edition* **48(42)**:7752-77.
3. Allen MJ, Tung VC. and Kaner RB. (2010) Honeycomb carbon: A review of graphene. *Chemical Review* **110**: 132–145.
4. Chabot V, Higgins D, Yu A, Xiao X, Chen Z, Zhang J. (2014) A review of graphene and graphene oxide sponge: material synthesis and applications to energy and the environment. *Energy and Environmental Science* **7(5)**:1564-96.
5. Szafrank BN., Fiori G, Schall D., Neumaier D. and Kurz H. (2012) Current saturation and voltage gain in bilayer graphene field effect transistors. *Nano Letters* **12**: 1324–8.
6. Xiong G, Meng C., Reifenberger RG, Irazoqui PP. and Fisher TS. (2014) A review of graphene-based electrochemical micro-supercapacitors. *Electroanalysis* **26**: 30–51.
7. Cong HP., Chen JF. and Yu SH. (2014) Graphene-based macroscopic assemblies and architectures: an emerging material system. *Chemical Society Reviews* **43**:7295–7325.
8. Wang X, Song M. (2013) Toughening of polymers by graphene. *Nanomaterials and Energy* **2**:265-278.
9. Wang ZG, Li PJ, Chen YF, He JR, Zheng BJ, Liu JB, Qi F. (2014) The green synthesis of reduced graphene oxide by the ethanol-thermal reaction and its electrical properties.

Materials Letters **116**:416-9.

10. Jiao Y., Zheng Y., Jaroniec M. and Qiao S. Z. (2014) Origin of the electrocatalytic oxygen reduction activity of graphene-based catalysts: A roadmap to achieve the best performance. *Journal of the American Chemical Society* **136**: 4394–4403.
11. Fasolino A, Los JH, Katsnelson MI. (2007) Intrinsic ripples in graphene. *Nature Materials* **6(11)**:858.
12. Loh KP, Bao Q, Ang PK. and Yang J. (2010) The chemistry of graphene. *Journal of Materials Chemistry* **20**: 2277.
13. Hao Y, Bharathi MS, Wang L, Liu Y, Chen H, Nie S, Wang X, Chou H, Tan C, Fallahazad B, Ramanarayan H. (2013) The role of surface oxygen in the growth of large single-crystal graphene on copper. *Science* **342**: 720–3.
14. Kim KS, Zhao Y, Jang H. Lee, SY. Kim, JM. Ahn, J.H. P. J.Y. Choi and Hong BH. (2009) Large-scale pattern growth of graphene films for stretchable transparent electrodes, *Nature* **457**:706-710.
15. Sutter PW, Flege JI, Sutter EA(2008) Epitaxial graphene on ruthenium. *Nature Materials* **7(5)**:406.
16. Kim N., Kuila T. and Lee J. (2013) Simultaneous reduction, functionalization and stitching of graphene oxide with ethylenediamine for composites application. *Journal of Materials Chemistry A* **1(4)**:1349-1358.
17. Das AK, Srivastav M, Layek RK, Uddin ME, Jung D, Kim NH, Lee JH. (2014) Iodide-mediated room temperature reduction of graphene oxide: a rapid chemical route for

- the synthesis of a bifunctional electrocatalyst. *Journal of Materials Chemistry A* **2(5)**:1332-40.
18. Gengler RY, Badali DS, Zhang D, Dimos K, Spyrou K, Gournis D, Miller RD. (2013) Revealing the ultrafast process behind the photoreduction of graphene oxide. *Nature Communications* **4**: 2560.
19. Pan Y, Wang S, Kee CW, Dubuisson E, Yang Y, Loh KP, Tan CH. (2011) Graphene oxide and rose bengal: oxidative C–H functionalization of tertiary amines using visible light. *Green Chemistry* **13 (12)**:3341-3344.
20. Ambrosi A., Chua C., Bonanni A. and Pumera M. (2014) Electrochemistry of graphene and related materials. *Chemical Reviews* **114(14)**:7150-7188.
21. Guo HL., Wang XF., Qian QY., Wang FB. and Xia X.-H. (2009) A Green approach to the synthesis of graphene nanosheets. *ACS Nano* **3**: 2653–2659.
22. Compton OC., and Nguyen ST. (2010) Graphene oxide, highly reduced graphene oxide, and graphene: Versatile building blocks for carbon-based Materials. *Small* **6**: 711–723.
23. Wang L, Park Y, Cui P, Bak S, Lee H, Lee SM, Lee H. (2014) Facile preparation of an n-type reduced graphene oxide field effect transistor at room temperature. *Chemical Communications* **50 (10)**:1224-1226.
24. Shin HJ, Kim KK, Benayad A, Yoon SM, Park HK, Jung IS, Jin MH, Jeong HK, Kim JM, Choi JY, Lee YH. (2009) Efficient reduction of graphite oxide by sodium borohydride and its effect on electrical conductance. *Advanced Functional Materials* **19(12)**:1987-92.

25. Pei S, Zhao J, Du J, Ren, W and Cheng, HM. (2010) Direct reduction of graphene oxide films into highly conductive and flexible graphene films by hydrohalic acids. *Carbon* **48**: 4466–4474.
26. Luo D, Zhang G, Liu J. and Sun X. (2011) Evaluation criteria for reduced graphene oxide. *Journal of Physical Chemistry C* **115**: 11327–11335.
27. Quintana, M., Vazquez, E., and Prato, M. (2013) Organic functionalization of graphene in dispersions. *Accounts of Chemical Research* **46**: 138–148.
28. Kuila T, Bose S, Khanra P, Mishra AK, Kim NH, Lee JH. (2012) A green approach for the reduction of graphene oxide by wild carrot root. *Carbon* **50(3)**:914-21.
29. Guo Y, Guo S, Ren J, Zhai Y, Dong S, Wang E. (2010) Cyclodextrin functionalized graphene nanosheets with high supramolecular recognition capability: synthesis and host–guest inclusion for enhanced electrochemical performance. *ACS Nano* **4(7)**: 4001-10.
30. Kuila T, Bose S, Mishra AK, Khanra P, Kim NH, Lee JH. (2012) Chemical functionalization of graphene and its applications. *Progress in Materials Science* **57(7)**:1061-105.
31. Zhang J, Yang H, Shen G, Cheng P, Zhang J, Guo S. (2010) Reduction of graphene oxide via L-ascorbic acid. *Chemical Communications* **46(7)**:1112-4.
32. Zhu C, Guo S, Fang Y, Dong S. (2010) Reducing sugar: new functional molecules for the green synthesis of graphene nanosheets. *ACS Nano* **4(4)**:2429-37.
33. Meyer JC, Geim AK, Katsnelson MI, Novoselov KS, Booth TJ, Roth S. (2007) The structure of suspended graphene sheets. *Nature* **446(7131)**:60-63.

34. Mhamane D, Ramadan W, Fawzy M, Rana A, Dubey M, Rode C, Lefez B, Hannoyer B, Ogale S. (2011) From graphite oxide to highly water-dispersible functionalized graphene by single step plant extract-induced deoxygenation. *Green Chemistry* **13(8)**:1990-6.
35. Singh TD, Singh TG and Henam SD (2017) Green synthesis, growth and catalytic activity of silver nanoparticles. *Green Materials* **5(4)**:165–172.
36. Tayade US, Borse AU, Meshram JS. (2017) Tailorable optical properties of silver nanoparticles from *Butea monosperma* plant extract. *Modern Organic Chemistry Research* **2(4)**:189-194.
37. Tayade US, Borse AU, Meshram JS. (2018) First report on *Butea monosperma* flower extract-based nickel nanoparticles green synthesis and characterization. *International Journal of Scientific Research in Science, Engineering and Technology* **4(3)**:41-47.
38. Choudhary BC, Paul D, Gupta T, Tetgure SR, Garole VJ, Borse AU, Garole DJ. (2017) Photocatalytic reduction of organic pollutant under visible light by green route synthesized gold nanoparticles. *Journal of Environmental Sciences* **1(55)**: 236-46.
39. Garole VJ, Choudhary BC, Tetgure SR, Garole DJ, Borse AU. (2018) Detoxification of toxic dyes using biosynthesized iron nanoparticles by photo-Fenton processes. *International Journal of Environmental Science and Technology* **15(8)**: 1649-56.
40. Kim KT, Dao TD, Jeong HM, Anjanapura RV, Aminabhavi TM. (2015) Graphene-coated with alumina and its utilization as a thermal conductivity enhancer for alumina sphere/thermoplastic polyurethane composite. *Materials Chemistry and Physics* **153**:291-300.

41. Bai S, Shen X. (2012) Graphene–inorganic nanocomposites. *RSC Advances* **2(1)**:64-98.
42. Koch KR. (1982) Oxidation by Mn_2O_7 : An impressive demonstration of the powerful oxidizing property of dimanganese-heptoxide. *Journal of Chemical Education* **59**: 973.
43. Aliofkhazraei M, Milne WI, Ozkan CS, Mitura S, Gervasoni JL, Ali N. (2016) Graphene science handbook: electrical and optical properties. *CRC press*.
44. Li J., Zeng X., Ren T. and van der Heide, E. (2014) The preparation of graphene oxide and its derivatives and their application in bio-tribological systems. *Lubricants* **2**: 137–161.
45. Menaga D, Rajakumar S, Ayyasamy PM. (2013) Free radical scavenging activity of methanolic extract of Pleurotus Florida mushroom. *International journal of pharmacy and pharmaceutical sciences* **5(4)**:601-6.
46. Stankovich S, Dikin DA, Piner RD, Kohlhaas KA, Kleinhammes A, Jia Y, Wu Y, Nguyen ST, Ruoff RS. (2007) Synthesis of graphene-based nanosheets via chemical reduction of exfoliated graphite oxide. *Carbon* **45(7)**:1558-65.
47. He J, and Giusti MM (2010) Anthocyanins: Natural colorants with health-promoting properties. *Annual Review of Food Science and Technology* **1**:163–187.
48. Khan M, Al-Marri AH, Khan M, Mohri N, Adil SF, Al-Warthan A, Siddiqui MR, Alkathlan HZ, Berger R, Tremel W, Tahir MN. (2014) Pulicaria glutinosa plant extract: a green and eco-friendly reducing agent for the preparation of highly reduced graphene oxide. *RSC Advances* **4(46)**:24119-25.
49. Guo, HL., Wang XF, Qian QY, Wang FB. and Xia XH (2009) A green approach to the synthesis of graphene nanosheets. *ACS Nano* **3**: 2653–2659.

50. Donawade DS, Raghu AV, Gadaginamath GS.(2006) Synthesis and antimicrobial activity of some new 1-substituted-3-pyrrolyl aminocarbonyl/oxadiazolyl/triazolyl/5-methoxy-2-methylindoles and benzo [g] indole. *Indian Journal of Chemistry* **45B**: 689-696.
51. Donawade DS, Raghu AV, Gadaginamath GS. (2007) Synthesis and antimicrobial activity of novel linearly fused 5-substituted-7-acetyl-2, 6-dimethyloxazolo [4, 5-f] indoles. *Indian Journal of Chemistry* **46B**: 690-693.
52. Mena P, Martí N, García-Viguera C. (2014) Varietal blends as a way of optimizing and preserving the anthocyanin content of pomegranate (*Punica granatum* L.) juices. *Journal of agricultural and food chemistry* **62(29)**:6936-43.
53. Qin CG, Li Y, Niu WN, Ding Y, Shang XY, and Xu CL. (2011) Composition analysis and structural identification of anthocyanins in fruit of waxberry. *Czech Journal of Food Sciences* **29(2)**:171-80.
54. Cong HP., Chen JF. and Yu SH. (2014) Graphene-based macroscopic assemblies and architectures: An emerging material system. *Chemical Society Reviews* **43**: 7295–7325.
55. Sett A, Gadewar M, Sharma P, Deka M, Bora U. (2016) Green synthesis of gold nanoparticles using aqueous extract of *Dillenia indica*. *Advances in Natural Sciences: Nanoscience and Nanotechnology* **7(2)**:025005.
56. Eda G, Lin YY, Mattevi C, Yamaguchi H, Chen HA, Chen IS, Chen CW, Chhowalla M. (2010) Blue photoluminescence from chemically derived graphene oxide. *Advanced Materials* **22(4)**:505-9.

57. Jamieson T, Bakhshi R, Petrova D, Pocock R, Imani M, Seifalian AM. (2007) Biological applications of quantum dots. *Biomaterials* **28(31)**:4717-32.
58. Kim J, Kim F, Huang J. (2010) Seeing graphene-based sheets. *Materials Today* **13(3)**:28-38.
59. Nilsson HM, de Knoop L, Cumings J, Olsson E. (2017) Localized resistance measurements of wrinkled reduced graphene oxide using in-situ transmission electron microscopy. *Carbon* **113**:340-5.
60. Naik GH, Priyadarsini KI, Satav JG, Banavalikar MM, Sohoni DP, Biyani MK, Mohan H. (2003) Comparative antioxidant activity of individual herbal components used in Ayurvedic medicine. *Phytochemistry* **63(1)**:97-104.
61. Pal, J., Ganguly, S., Tahsin, K. and Acharya, K. (2010) In vitro free radical scavenging activity of wild edible mushroom, *Pleurotus squarrosulus* (Mont.) Singer. *Indian Journal of Experimental Biology* **48(12)**: 1210-1218.
62. Saikia JP, Paul S, Konwar BK, Samdarshi SK. (2010) Nickel oxide nanoparticles: a novel antioxidant. *Colloids and Surfaces B: Biointerfaces* **78(1)**:146-8.
63. Sathiyamoorthi E, Iskandarani B, Salunke BK, Kim BS. (2018) Bio-medical potential of silver nanoparticles biosynthesized using gallnut extract. *Green Materials* **4**:1-0.

Table 1. Phytochemical screening of *Punica grantum* L. seed extract

Sr.no.	Type of test	Procedure	Observation	Presence/ Absence
1	Test for Amino acid A] Ninhydrin test	Ninhydrin solution + 2ml plant extract	Purple color	-
2	Test for Carbohydrates A] Molish test	Plant extract +1-naphthol+ conc. sulphuric acid	Violet ring	+
3	Test for fixed Oils and Fats A] Spot test	Spot the drop of plant extract	Oil stain	-
4	Test for Glycosides A] Borntragers test	2ml plant extract+ 3ml of Chloroform+ 10% ammonia solution	Pink color	+
5	Test for Phenolic compound A] Ferric Chloride test	Plant extract + few drops of 5 % neutral FeCl ₃	Green color	+
	B] Lead acetate test	Plant extract + few drops of lead acetate	White precipitate	+
6	Test for Flavonoids compound A] Alkaline reagent test	2ml plant extract+ ammonium hydroxide solution	Yellow Fluorescence	+
	Test for Phytosterols A] Liberman-Burchards test	Plant extract + acetic anhydride+ Conc.sulphuric acid	Sharp color change	+
8	Test for Proteins A] Biuret test	Plant extract + copper sulphate solution+ KOH solution	Pink color	+
9	Test for Saponins	Plant extract + distilled water	Foam formation	-
10	Test for gum and Mucilage's	Plant extract + ethanol	White precipitate	-

Table 2. Bandgap value of dispersing solvent

Solvents	Graphene oxide	Reduced graphene oxide
Ethylene glycol	2.78	2.62
Ethanol	4.62	4.32

Figure 1. Graphical abstract containing Punica granatum L seed extraction and graphene oxide reduction

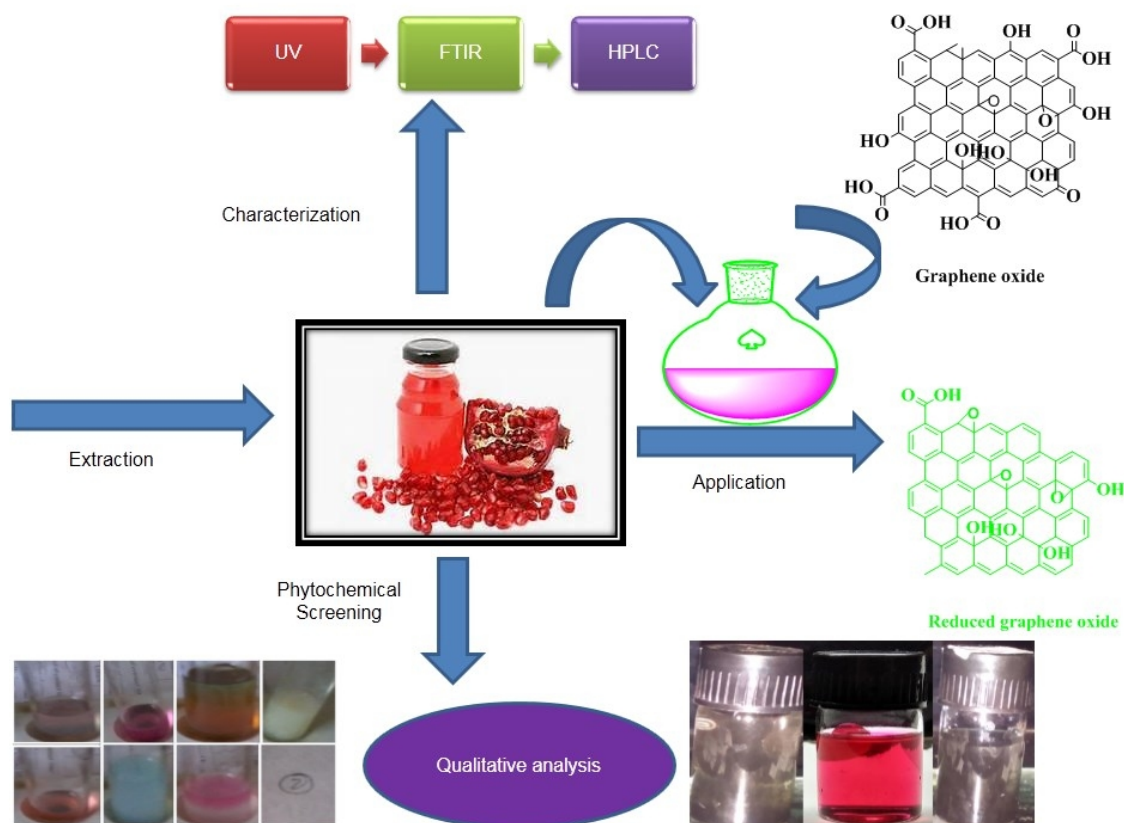


Figure 2. A plausible mechanism of reduction of graphene oxide

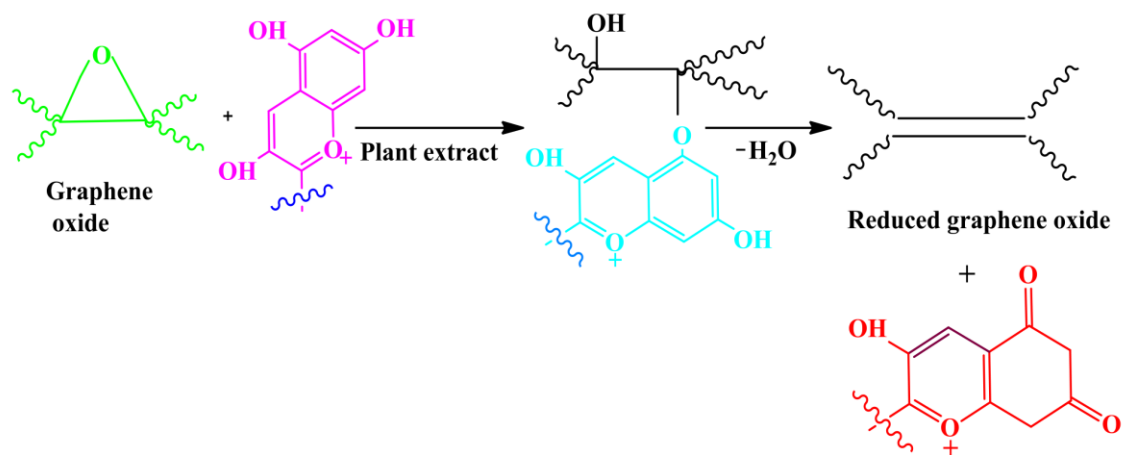


Figure 3. UV-Visible spectra of a) Graphene oxide b) Reduced graphene oxide c) Punica granatum L seed extract

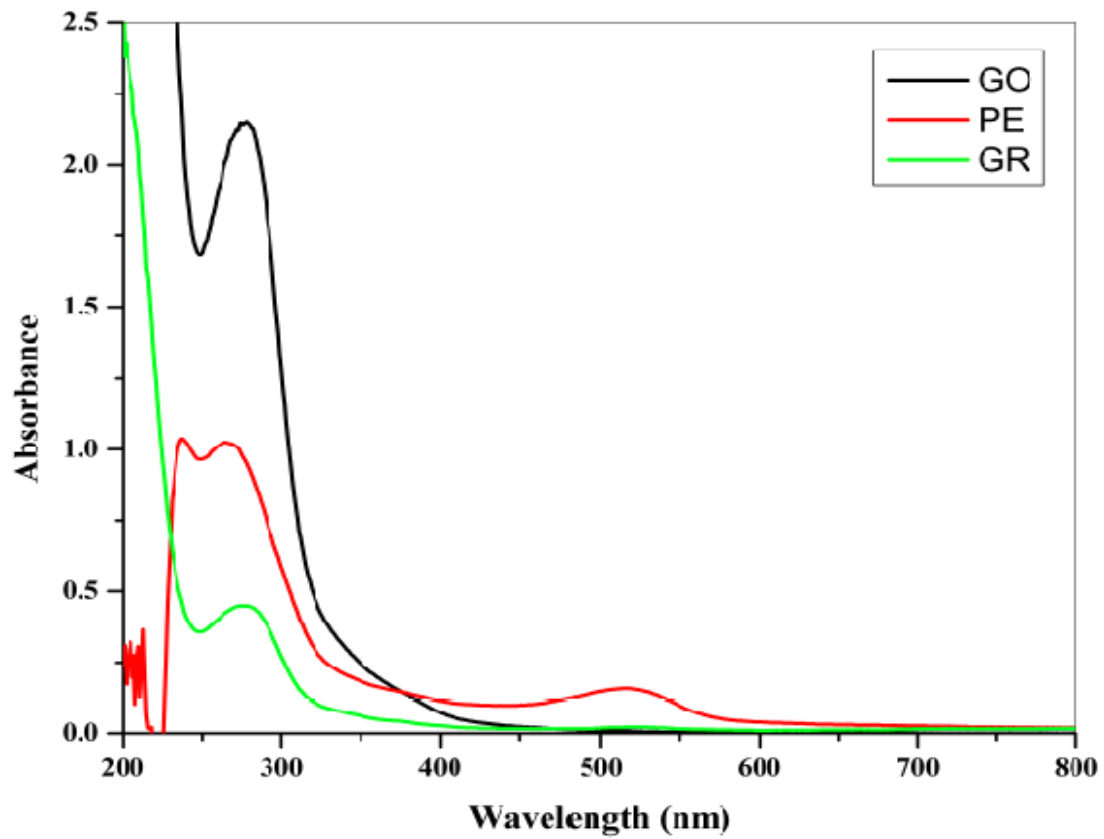
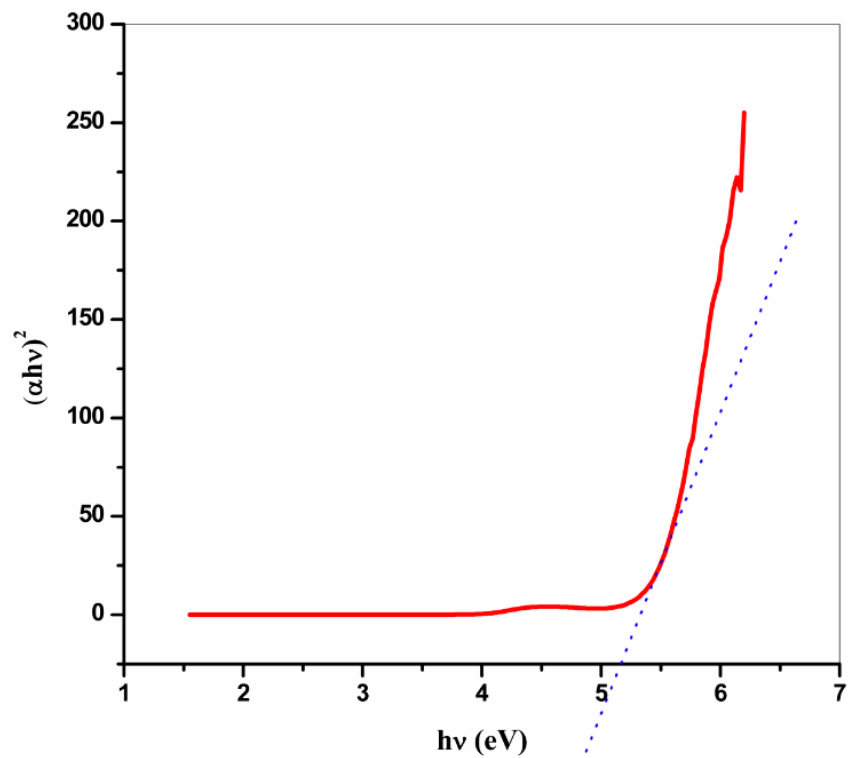
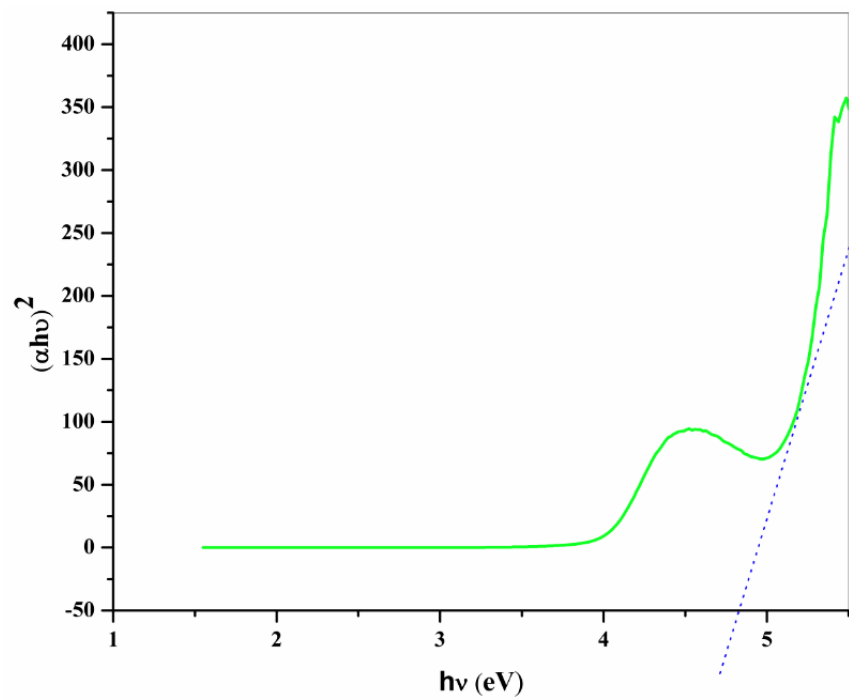


Figure 4. The band gap of a) Graphene oxide b) Reduced graphene oxide by Tauc plot



(a)



(b)

Figure 5. FT-IR spectra of a) Graphite b) Graphene oxide c) Reduced Graphene oxide d) Punica grantum L seed extract

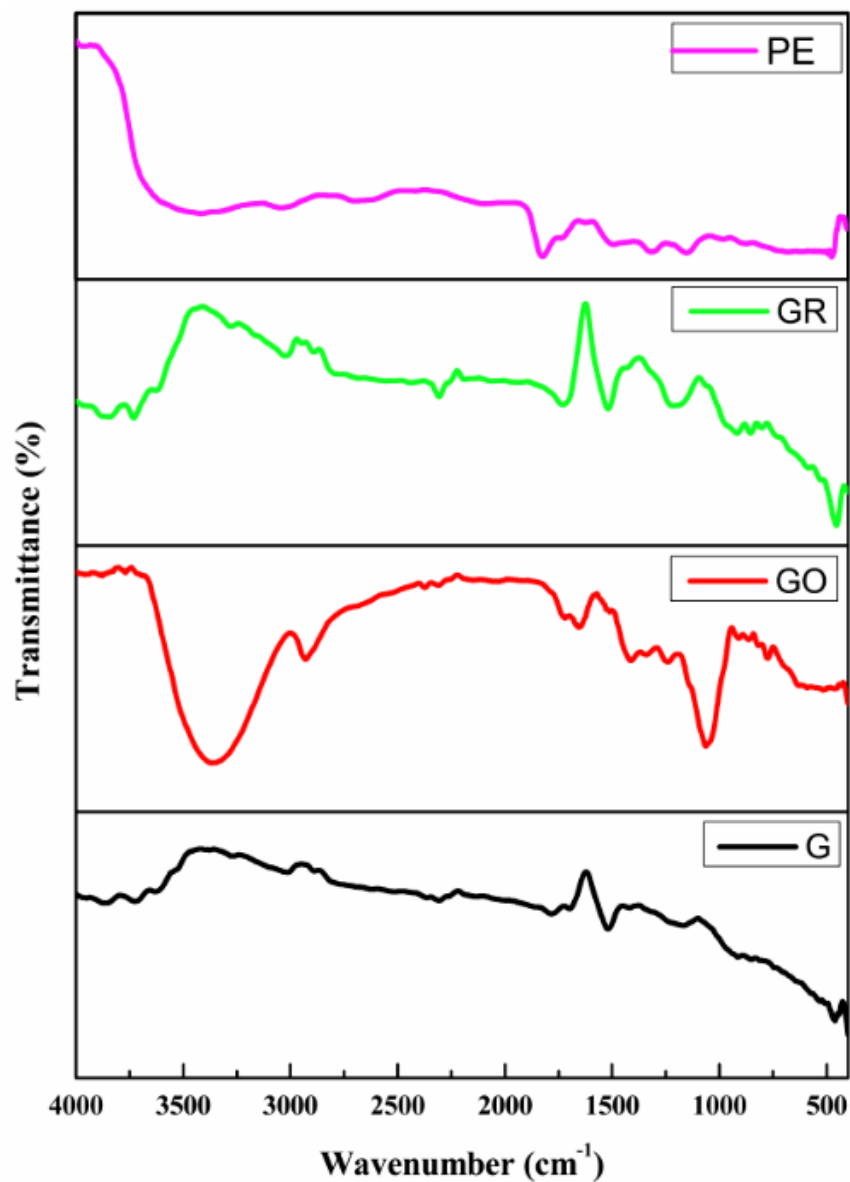
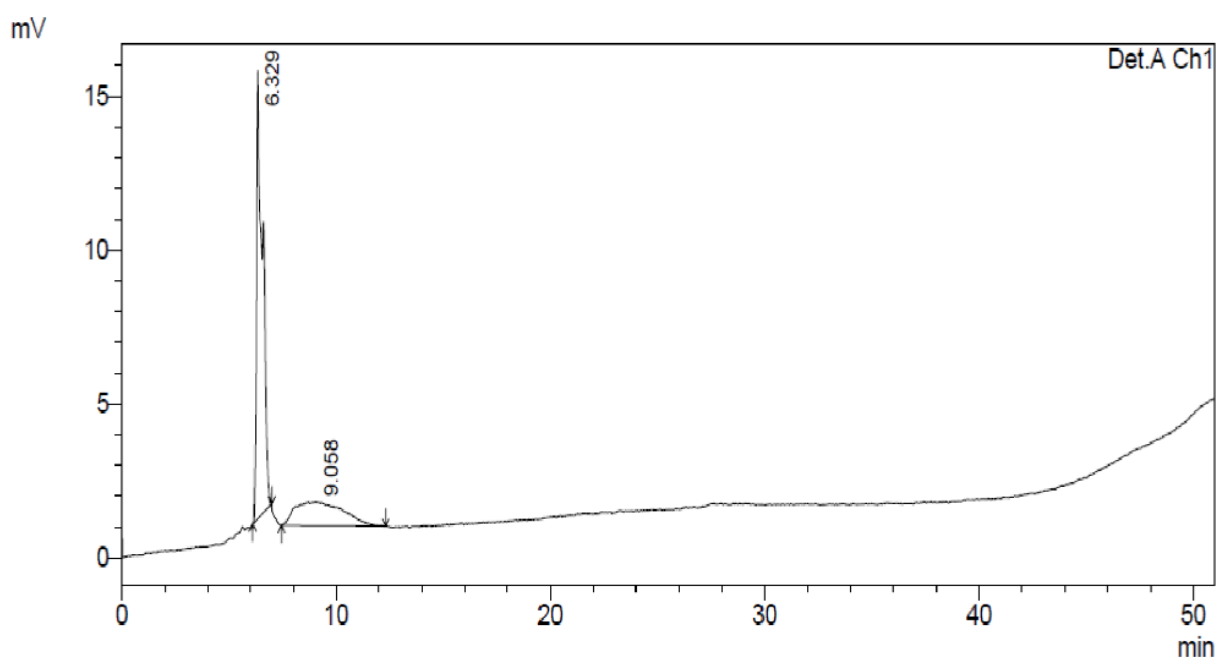


Figure 6. HPLC of *Punica granatum* L seed extract



1Det.A Ch1/520nm

<Results>

Detector A Ch1 520nm

Peak #	Ret. Time	Area	Height	Area %	Height %	Mark
1	6.329	291183	14558	70.727	94.978	
2	9.058	120519	770	29.273	5.022	
Total		411702	15328	100.000	100.000	

Figure 7. XRD pattern of a) Graphite b) Graphene oxide c) Reduced graphene oxide

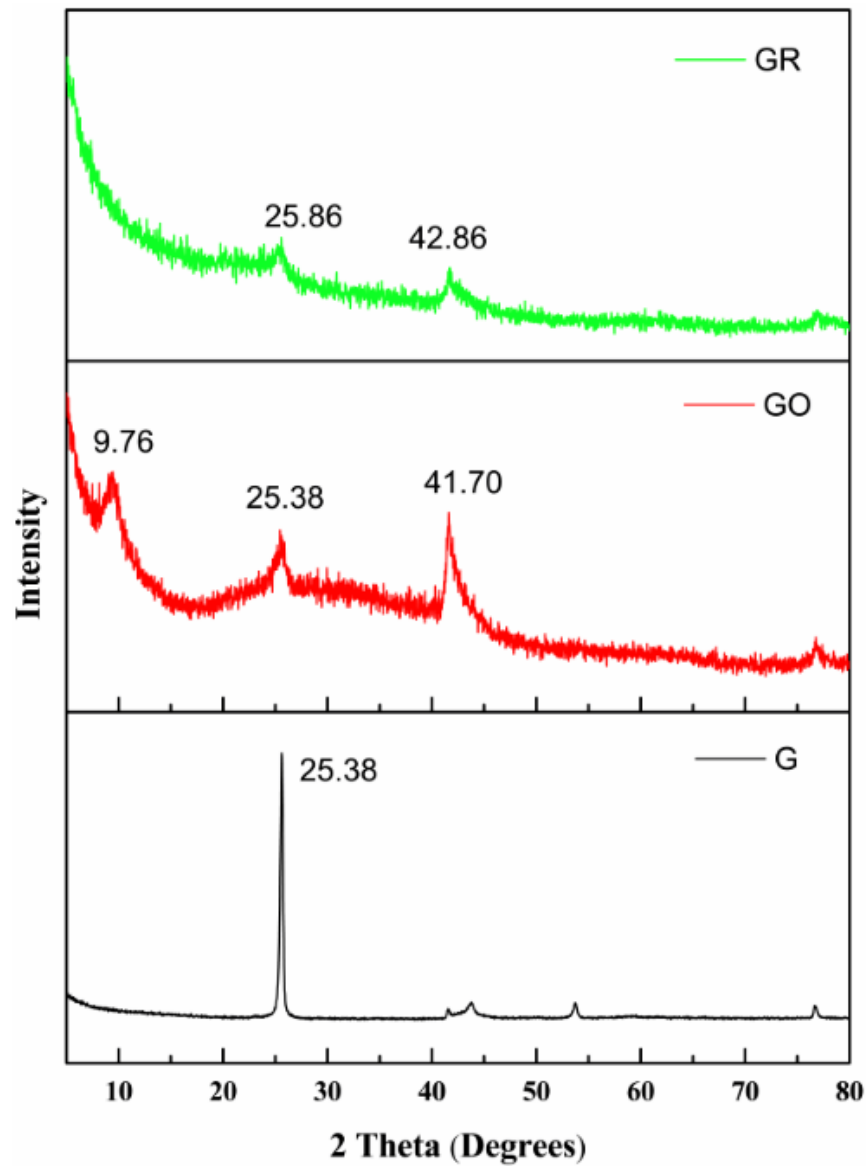


Figure 8. Raman spectra of a) Graphite b) Graphene oxide c) Reduced graphene oxide

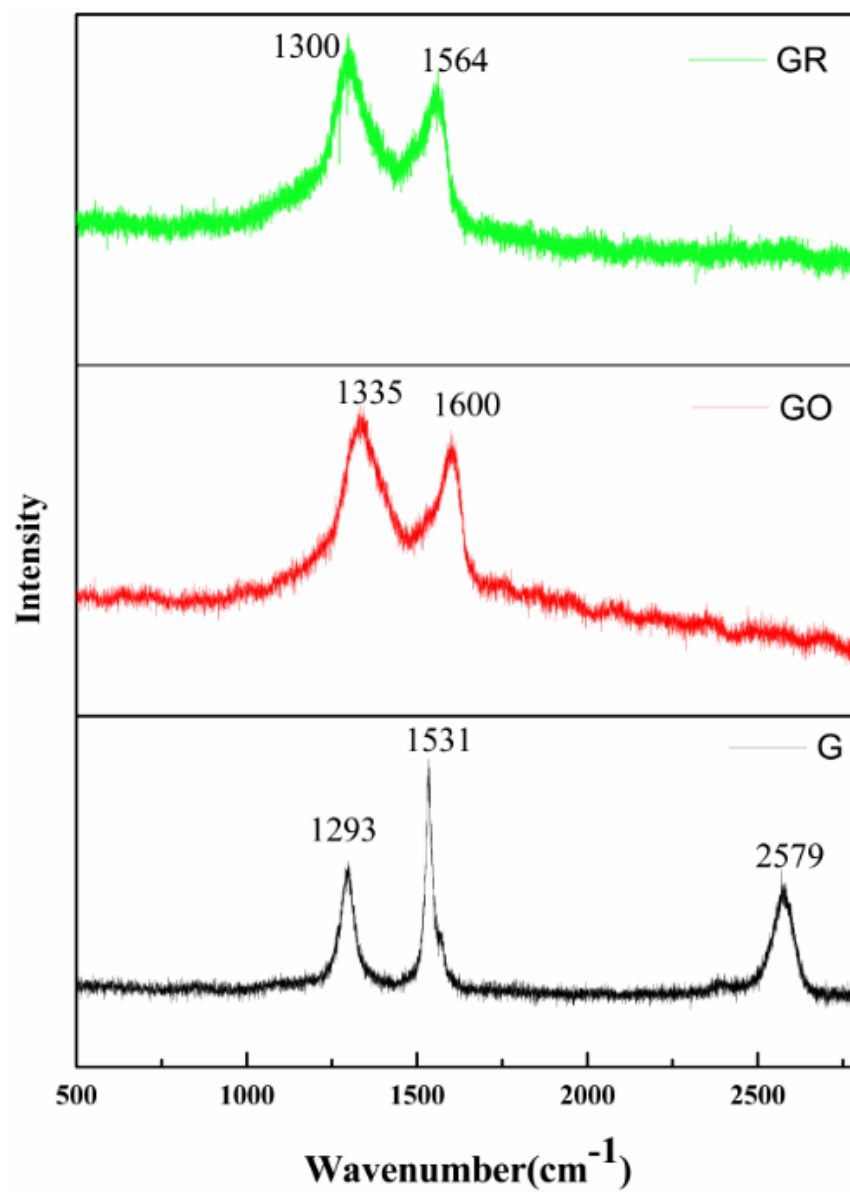
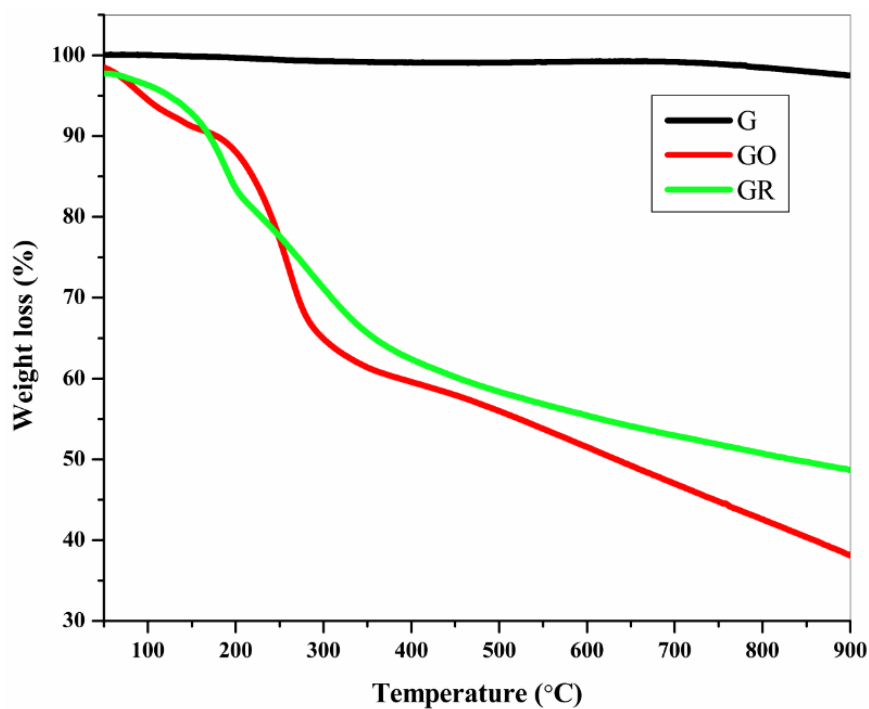
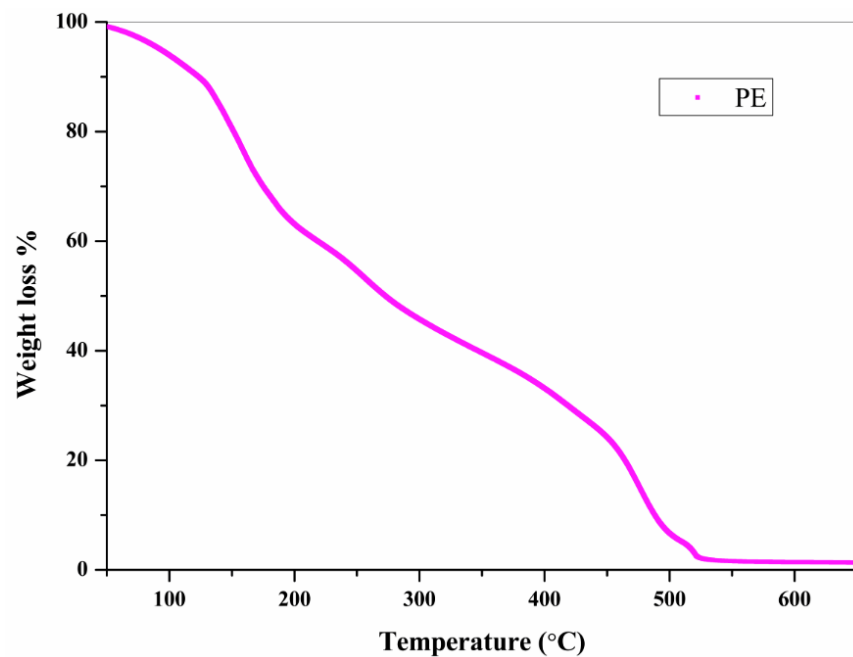


Figure 9. A) Thermogravimetric analysis of a] Graphite b] Graphene oxide c] Reduced graphene oxide. B) Thermogravimetric analysis of Punica grantum L. seed extract



(A)



(B)

Figure 10. Scanning electron microscopy of a) Graphite b) Graphene oxide c) Reduced graphene oxide d) Particle size in nano-sheets of reduced graphene oxide

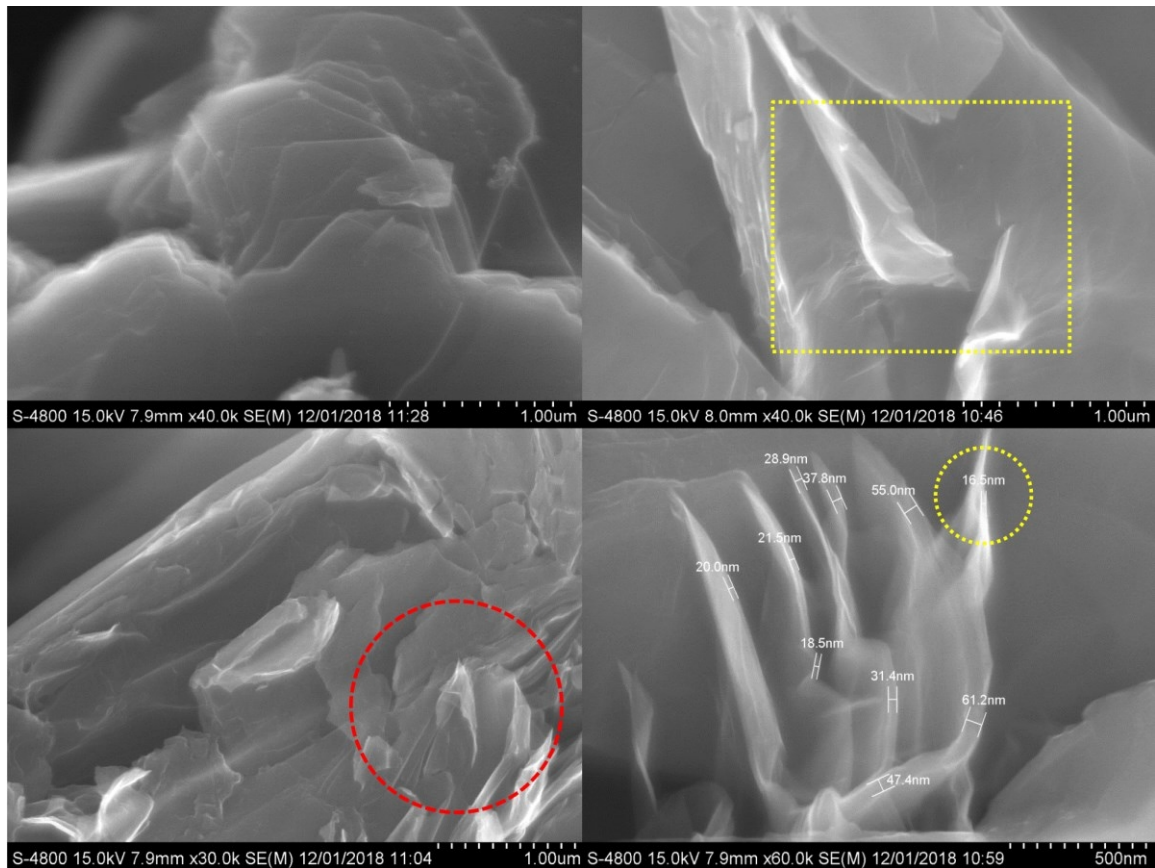
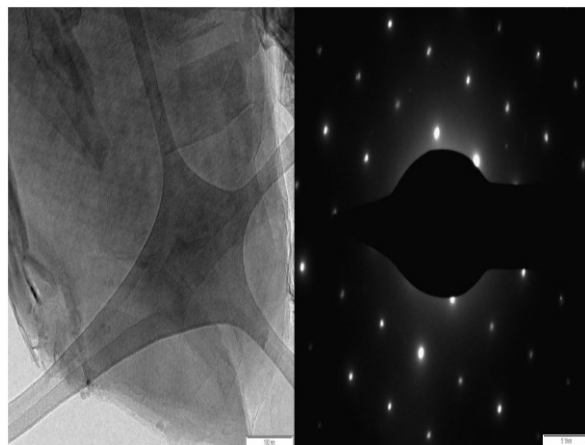
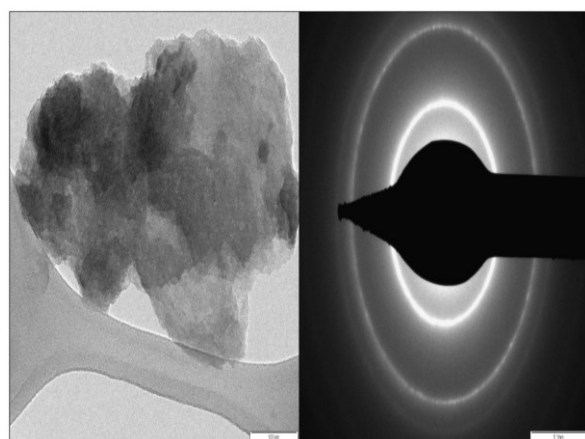


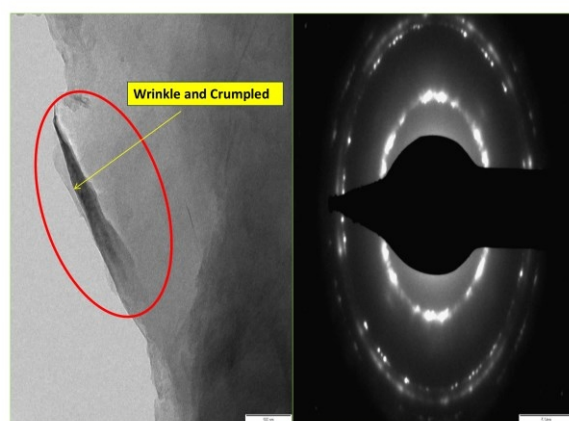
Figure 11. Transmission electron microscopy and Selected area electron diffraction of a) Graphite b) Graphene oxide c) Reduced graphene oxide



(a)

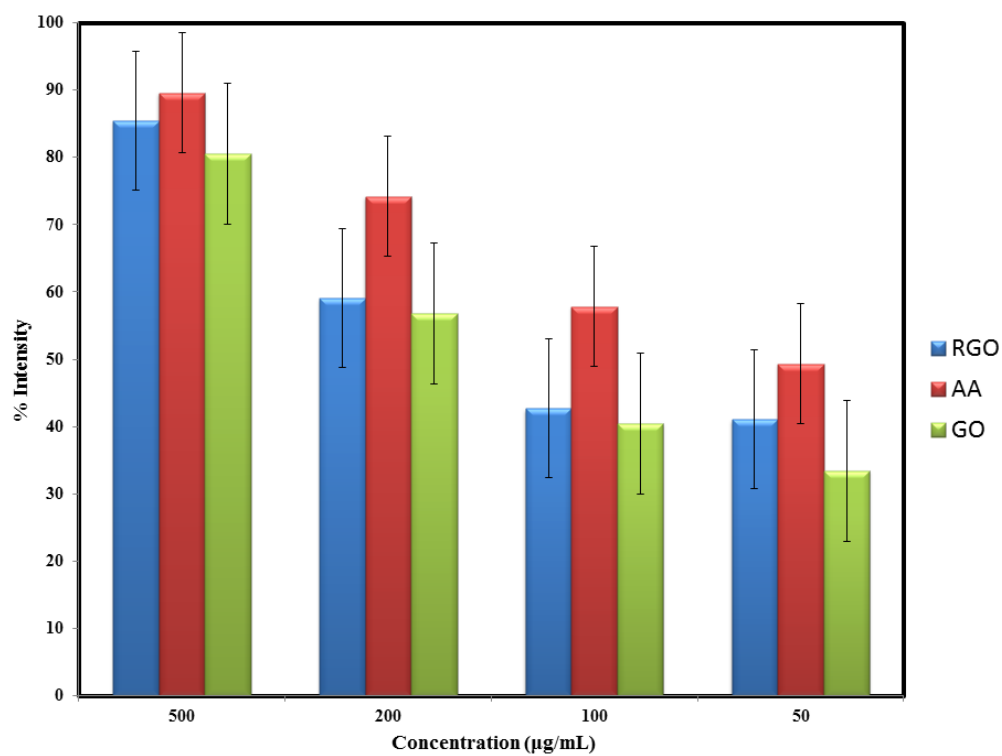


(b)



(c)

Figure 12. Antioxidant activity of a) Graphene oxide b) Reduced graphene oxide and Ascorbic acid



Tailor Able Optical Properties of Silver Nanoparticles from Butea Monosperma Plant Extract

Ujwala S. Tayade¹, Amulrao U. Borse^{1*}, Jyotsna S. Meshram^{2*}

¹School of Chemical Sciences, North Maharashtra University, Jalgaon (M.S.), India

²Department of Chemistry, Rashtrasant Tukadoji Maharaj University, Nagpur (M.S.), India
Email: drjsmeshram@gmail.com, amulborse@gmail.com

Abstract. Nowadays Silver nanoparticles are in increasing commercial demands due to their enormous application in wide range of scientific fields, such as medicines, catalysis, electronics, chemistry and energy. Herein we have reported a very simple and green approach of chemical reduction method for nanoparticle synthesis. The plant extract of Butea monosperma is used as reducing agent as well as capping agent. For confirmation of essential phytochemicals present in extract screening of phytochemicals such as Proteins, Flavonoids, Terpenoids, Cardiac glycosides and Tannins etc. has been carried out in the present study. The UV- Visible spectroscopy has been used to determine Surface Plasmon Resonance (SPR) and Infrared Spectroscopy (IR) to confirm functional groups. From the Absorbance the band gap values have been calculated which are useful in soft electronic devices.

Keywords: Green approach, capping agent, phytoconstituent, surface plasmon resonance, band gap

1. Introduction

The role of plant materials as medicines owing the presence of crucial Phytoconstituent and the specific action to cure various diseases without affecting the other organs plays a crucial role in Science, research and development. The nanotechnology research focusing on plant materials used to synthesis of nanomaterial is on rise. The particles with size were less than 100 nm, Nanoparticles (NPs). Entirely novel and enhanced characteristics such as size, distribution and morphology are revealed by these particles in comparison to the larger particles of the bulk material from which they can be prepared [1]. Nanoparticles of noble metals like gold, silver and platinum are well - recognized to have significant applications in electronics, magnetic, optoelectronics and information storage devices [2-5]. One such important member of the noble metal NPs are silver (Ag NPs), widely used in shampoos, soaps, cosmetics, toothpastes, medicinal and pharmaceutical products [6, 7]. The universal demand of silver nanoparticles is larger than the production rate and the pioneering ideas are more promising for nanoparticles synthesis such as more economic and sustainable routes (Green methods of nanoparticles synthesis). Different approaches available for the synthesis of silver nanoparticles are chemical [8], electrochemical [9], radiation [10], photochemical methods [11] and bio based methods [12-14]. All mentioned techniques of silver NPs preparation, plant-mediated bio mimetic synthesis of silver nanoparticle is considered a widely use technology or rapid production of silver nanoparticles for successfully obtaining the excessive need and current market demand and resulting reduction of harmful chemicals in synthesis of nanoparticles. Studies have shown that Alfalfa roots can absorb Ag (0) from agar medium and able to transport it to the plant shoot in the same state of oxidation [15]. Ag NPs were also obtained using *Jatropha curcas* [16], *Aloe Vera* [17], *Acalypha indica* [18], *Garcinia mangostana* leaf extracts [19], *Crataegus douglasii* fruit extract [20] as well as wide range of other plant extracts [21] as reducing agent. Herein we have developed a rapid, eco-friendly and convenient green method for the synthesis of silver nanoparticles from silver nitrate using Butea monosperma plant extract as a reducing agent and capping agent merely at room temperature. Ag NPs were characterized and studied in details with all of their properties significant to current science and prevailing technologies. Silver nanoparticles have attracted more and more attention because of their fascinating electrical, thermal and optical

properties. Silver has the highest electrical conductivity (6.3×10^7 S/m) among all the metals, by virtue of which Ag Nanoparticles are considered as very promising candidates in flexible electronics [22-24].

2. Methods

Preparation of the leaf extract

The Indian medicinal plant, *Butea monosperma* is selected from Maharashtra, India because of its cost effectiveness, ease of availability and medicinal properties. Fresh and healthy flowers were collected locally and rinsed thoroughly first with tap water followed by distilled water to remove all the dust and unwanted visible particles, cut into small pieces and dried at room temperature. About 10 gm. of these finely incised flowers of plant type were weighed separately and transferred into 250 mL flask containing 100 mL distilled water and boiled for about 10 min. The extract was then filtered thrice through Whatman No. 1 filter paper to remove particulate matter and to get clear solution which was then refrigerated (4°C) for further experiments. In each step of the experiment, sterility conditions were maintained for the effectiveness and accuracy in results without contamination.

3. Phytochemical Analysis

Qualitative Analysis

Following standard protocols were used for qualitative analysis of samples to check for the presence of Alkaloids, Carbohydrates, Cardiac glycosides, Flavonoid, Phenols, Saponins, Tannins, Terpenoids, Quinones and Proteins respectively.

1. Test for Flavonoids: 2 ml of each extract was added with few drops of 20% sodium hydroxide, formation of intense yellow colour is observed. To this, few drops of 70% dilute hydrochloric acid were added and yellow colour was disappeared which indicates the presence of flavonoids in the sample extract.

2. Test for Alkaloids: To 1 ml of each extract, 1 ml of marquis reagent, 2ml of concentrated sulphuric acid and few drops of 40% formaldehyde were added and mixed, appearance of dark orange or purple colour indicates the presence of alkaloids.

3. Test for Saponins: To 2 ml of each extract, 6 ml of distilled water were added and shaken vigorously; formation of bubbles or persistent foam indicates the presence of Saponins.

4. Test for Tannins: To 2 ml of each extract, 10% of alcoholic ferric chloride was added; formation of brownish blue or black colour indicates the presence of tannins.

5. Test for Phenols: To 2 ml of each extract, 2 ml of 5% aqueous ferric chloride was added; formation of blue colour indicates the presence of phenols in the sample extract.

6. Test for Proteins: To 2 ml of each extract, 1 ml of 40% sodium hydroxide and few drops of 1% copper sulphate were added; formation of violet colour indicates the presence of peptide linkage molecules in the sample extract.

7. Test for Cardiac Glycosides: To 1 ml of each extract, 0.5ml of glacial acetic acid and 3 drops of 1% aqueous ferric chloride solution were added and formation of brown ring at the interface indicates the presence of cardiac glycosides in the sample extract.

8. Test for Terpenoids: Take 1 ml of extract of each solvent and add 0.5 ml of chloroform followed by a few drops of concentrated sulphuric acid, formation of reddish brown precipitate indicates the presence of Terpenoids in the extract.

9. Test for Carbohydrates: Take 1 ml of extract, add few drops of Molish reagent and then add 1 ml of concentrated sulphuric acid at the side of the tubes. The mixture was then allowed to stand for 2 to 3 minutes. Formation of red or dull violet colour indicates the presence of carbohydrates in the sample extract.

4. Preparation of Silver Nanoparticles Using *Butea Monosperma* Extract

Aqueous solution (1mM) of Silver nitrate (AgNO_3) and leaf extract was added for the reduction of Ag ions. The mixture was kept on Magnetic Stirrer for 30 min at room temperature. In the meantime, colour change of the mixture from faint light to yellow- brown to colloidal brown was monitored

periodically (time and colour change was recorded along with periodic sampling and scanning by UV-Visible Spectrometer) for maximum 30 min(Figure 1) .The reaction was carried out in darkness to avoid photo activation of AgNO_3 at room temperature. After formation of Ag Nanoparticles centrifugation was carried at 3200 rpm for 10 min washed twice with deionized water to remove any impurities present.

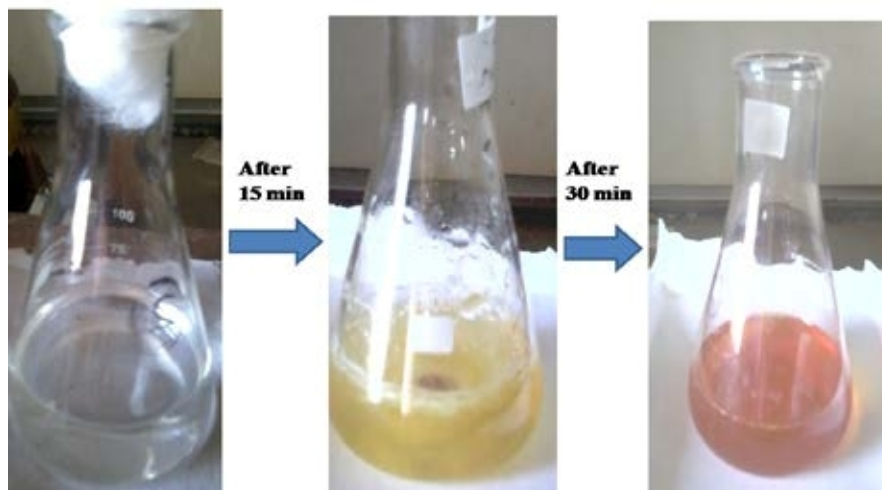


Figure 1. Synthesis of silver nanoparticles

Instrumentation

Infrared spectroscopy (FT-IR) was measured on a Shimadzu FTIR-8400 spectrometer 400cm^{-1} to 4000cm^{-1} at room temperature. The Ultra Violet-Visible spectroscopy (UV-Vis) absorption study was performed at room temperature in the wavelength range of 200–800 nm on a UV-Vis spectrometer Shimadzu UV-1700.

5. Characterization

UV-Visible analysis (Figure 2 & Figure 3)

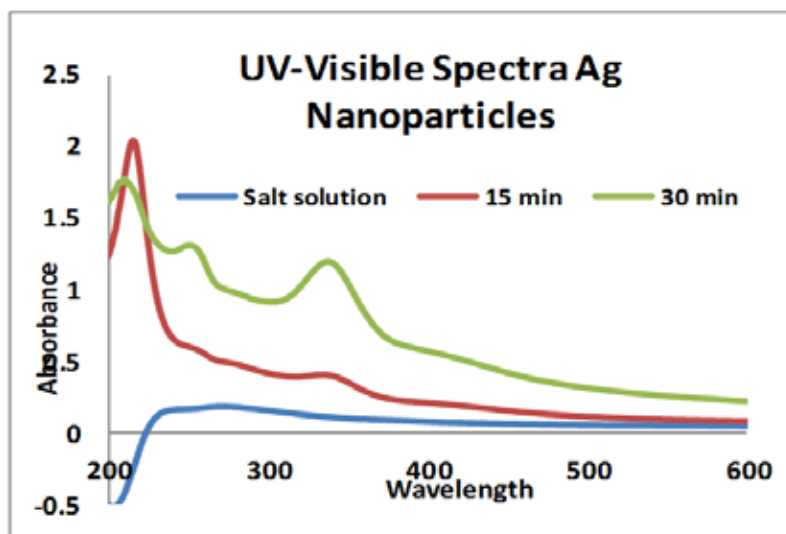


Figure 2 UV-visible analysis of silver nanoparticles

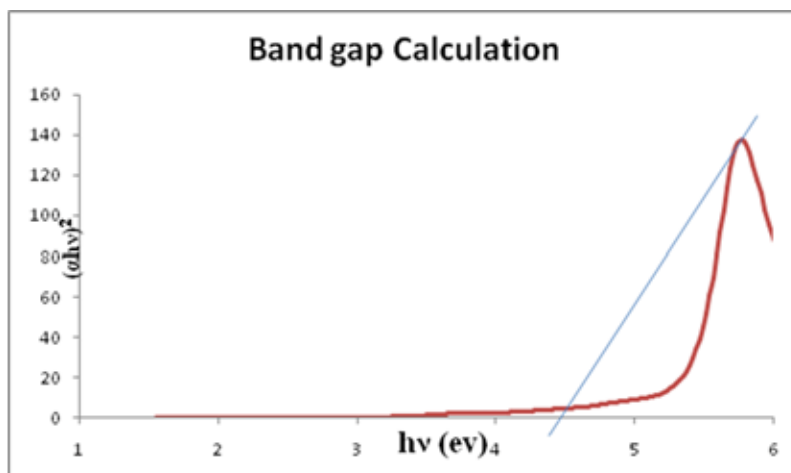


Figure 3 Band gap calculation of silver nanoparticles

FTIR analysis (Figure 4)

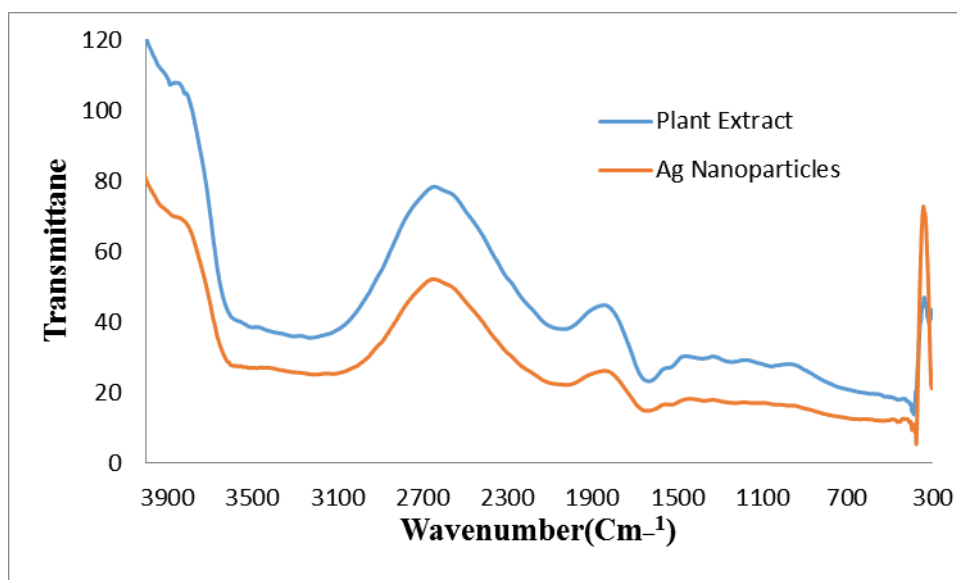


Figure 4 FTIR analysis of silver nanoparticles

Phytochemical Screening (Table 1)

Table 1 Phytochemical screening

Sr.no.	Phytochemicals test	Procedure	Present /Absent
1	Carbohydrates	Plant extract + 1-naphthol + Conc.Sulphuric acid	-
2	Protein	Plant extract + copper sulphate solution + KOH solution	+
3	Alkaloids	Plant extract + Meyers Reagent	-
4	Flavonoid	2ml plant extract + ammonium hydroxide solution	+
5	Terpenoids	2ml plant extract+ Chloroform + Conc. sulphuric acid	+
6	Cardiac Glycosidase	2ml plant extract+ 3ml of Chloroform+ 10% ammonia solution	+
7	Tannins	Plant extract + few drops of lead acetate	+
8	Saponins	Plant extract + distilled water	-

6. Results and Discussion

In this plant extract performing the various tests for phytochemical screening which indicates existence of Proteins, Flavonoids, Terpenoids, Cardiac Glycosidase and Tannins etc. plays more fundamental role in bio based nanoparticles synthesis.

6.1 UV-Visible Spectral Analysis

The Bio based reduction of Silver in the reaction mixture monitored by periodic sampling at regular interval by UV-Visible Spectroscopy. The metal ion solution does not show any change in its absorbance also not largest. But the reaction mixture at 15 and 30 min respectively shows 340nm and 420 nm which is Characteristic values of Silver nitrate solution and Surface Plasmon Resonance Analysis by Spectrophotometer was made up to 30 min.

6.2 Band Gap Calculation

The band gap value of Silver nanoparticles can be calculated by using following equation,

$$E_g = 1240 / \lambda \quad (1)$$

The band gap Value comes out which is 4.36 eV.

6.3 Fourier Transfer Infrared Spectroscopy

Some functional groups in silver nanoparticles are confirmed by FTIR analysis. The band values at 3398 cm^{-1} , characteristic of -OH and -NH Vibrational frequencies. Vibrational peaks between 2899 and 2977 cm^{-1} were characteristic frequency of -CH Symmetrical vibration of saturated hydrocarbons. The Vibrational frequency of C-O observed in the spectra of the extract at 1047 and 1087 cm^{-1} . Deviation from this region to higher wavenumber was observed indicating secondary amide. The peaks were sharper than the frequency of -OH peaks due to reduction in hydrogen bonds which increased with electro negativity. The sharp peak observed below 500 cm^{-1} indicates presence of silver nanoparticles formation.

7. Conclusion

In this work extract of Butea monosperma plants carried out and their phytochemical analysis was also carried which indicates the presence of Proteins, Flavonoids, Terpenoids, Cardiac Glycosidase and Tannins etc. plays more fundamental role in bio based nanoparticles synthesis. The synthesized nanoparticles show good optical properties and tailor ability for applications having band gap value 4.36 eV. It is very simple and less time - consuming method of nanoparticles synthesis.

References

1. Van den Wildenberg W. Roadmap report on nanoparticles. Wand W Espan Barcelona, *Spain*, Vol.57. 2005.
2. M. Grätzel Photo electrochemical cells. *Nature*, Vol.414, pp.338-44, 2001.
3. M.Okuda, Y., Kobayashi, K. Suzuki, K.Sonoda, T.Kondoh, A.Wagawa, A. Kondo and H.Yoshimura, "Self-organized inorganic nanoparticle arrays on protein lattices," *Nano letters*, Vol.5, pp.991-993, 2005.
4. J. Dai and M.L.Brueening,"Catalytic nanoparticles formed by reduction of metal ions in multilayered polyelectrolyte films," *Nano Letters*, Vol.2, pp.497-501, 2002.
5. C.B.Murray, S.Sun, Doyle and T.Betley,"Mon disperse 3d transition-metal (Co, Ni, Fe) nanoparticles and their assembly into nanoparticle super lattices," *Materials Bulletin*, Vol.26, pp.985-991, 2001.
- 6.R.Bhattacharya and P.Mukherjee, "Biological properties of naked metal nanoparticles," *Advanced drug delivery reviews*,Vol.60,pp.1289-1306, 2008.
7. D.R.Bhumkar, H.M.Joshi, M.Sastry and V.B.Pokharkar, "Chitosan reduced gold nanoparticles as novel carriers

- for trans mucosal delivery of insulin," *Pharmaceutical research*, Vol.24, pp.1415-1426, 2007.
8. Y.Sun, Y. Yin, B.T. Mayer's, T. Herrick's and Y. Xia, "Uniform silver nanowires synthesis by reducing AgNO₃ with ethylene glycol in the presence of seeds and poly (vinyl pyrrolidone)," *Chemistry of Materials*, Vol.14, pp.4736-4745, 2002.
 9. B.Yin, H.Ma. S. Wang and S.Chen, "Electrochemical synthesis of silver nanoparticles under protection of poly (N-vinylpyrrolidone)," *The Journal of Physical Chemistry B*, Vol.107, pp.8898-8904, 2003.
 - 10.N.M.Dimitrijevic, D.M.Bartels, C.D.Jonah, K.Takahashi and T.Rajh, "Radiolytically Induced Formation and Optical Absorption Spectra of Colloidal Silver Nanoparticles in Supercritical Ethane," *The Journal of Physical Chemistry B*, Vol.105, pp.954-959, 2001.
 11. A.Callegari, D. Tonti, and M.Chergui, "Photo chemically grown silver nanoparticles with wavelength-controlled size and shape," *Nano Letters*, Vol 3, pp.1565-1568, 2003.
 12. L.Zhang, Y.Shen, A.Xie, B. Jin and Q.Zhang, "One-step synthesis of mono disperse silver nanoparticles beneath vitamin E Langmuir monolayers," *The Journal of Physical Chemistry B*, Vol 110, pp.6615-6620, 2006.
 13. A.Swami, P.R.Selvakannan, R.Pasricha and M.Sastry, "One-step synthesis of ordered two-dimensional assemblies of silver nanoparticles by the spontaneous reduction of silver ions by pentadecyl phenol Langmuir monolayers," *The Journal of Physical Chemistry B*, Vol 108, pp.19269-19275, 2004.
 14. R.R.Naik, S.J.Stringer, G.Agrwal, S.E.Jones and M.O.Stone, "Biomimetic synthesis and patterning of silver nanoparticles," *Nature materials*, Vol 1, pp.169-172, 2002.
 15. J.L.Gardea-Torresdey, J.G.Parsons, H.Troiani and M.Jose-Yacaman, "Alfalfa sprouts: a natural source for the synthesis of silver nanoparticles," *Langmuir*, Vol 19, pp.1357-1361, 2003.
 16. H.Bar, D.K. Bhui, G.P.Sahoo, P. Sarkar and A.Misra, "Green synthesis of silver nanoparticles using latex of *Jatropha curcas*," *Colloids and surfaces A: Physicochemical and engineering aspects*, Vol 339, pp.134-139, 2009.
 17. S.P.Chandran, M. Chaudhary, R.Pasricha, A.Ahmad and M.Sastry, "Synthesis of gold Nano triangles and silver nanoparticles using Aloe Vera plant extract," *Biotechnology progress*, Vol 22, pp.577-583, 2006.
 - 18.C.Krishnaraj, E.G.Jagan, S. Rajasekar, P. Selvakumar, and N.Mohan, "Synthesis of silver nanoparticles using *Acalypha indica* leaf extracts and its antibacterial activity against water borne pathogens," *Colloids and Surfaces B: Bio interfaces*, Vol 76, pp.50-56,2010.
 - 19.T.Z.Xin, N.Jeyakumar and S.A.Dhanaraj, "Biosynthesis of silver nanoparticles using mangos teen leaf extract and evaluation of their antimicrobial activities," *Journal of Saudi Chemical Society*, Vol 15, pp.113-120, 2011.
 20. Ghaffari-Moghaddam and Hadi-Dabanlou, "Plant mediated green synthesis and antibacterial activity of silver nanoparticles using *Crataegus douglasii* fruit extract," *Journal of Industrial and Engineering Chemistry*, Vol 20, pp.739-744, 2014.
 21. M.Ghaffari-Moghaddam, R. Hadi-Dabanlou, M.Rakhshanipour and K.Shameli, "Green synthesis of silver nanoparticles using plant extracts," *Korean Journal of Chemical Engineering*, Vol 31, pp.548-557, 2014.
 22. D.Azulai, T.Belenkova, H.Gilon, Z. Barkay and G.Markovich, "Transparent metal nanowire thin films prepared in mesostructured templates," *Nano letters*, Vol 9, pp.4246-4249, 2009.
 23. Y.Sun, "Silver nanowires—unique templates for functional nanostructures," *Nano scale*, Vol 2, pp.1626-1642, 2010.
 24. S.De, P.E. Lyons, E.M. Doherty, Nirmalraj, J.J.Boland and J.N.Coleman, "Silver nanowire networks as flexible, transparent, conducting films: extremely high DC to optical conductivity ratios," *ACS Nano*, Vol 3, pp.1767-1774, 2009.